

# EXIT Chart Analysis of Turbo-BLAST Receivers in Rayleigh Fading Channels

Wenjun Li and Huaiyu Dai

Department of Electrical and Computer Engineering  
North Carolina State University, Raleigh, NC 27606  
Email: Wli5@ncsu.edu, Huaiyu.Dai@ncsu.edu

**Abstract**—Turbo-BLAST is an advanced space-time layered architecture developed to approach capacity limit of multiple-input multiple-output (MIMO) systems. In a recent work [1], various multiuser detection (MUD) techniques have been explored in conjunction with Turbo-BLAST to combat the co-channel interference (CCI) and significantly improve the performance of MIMO systems in a multicell structure. In this paper, we study the extrinsic information transfer (EXIT) functions of several such Turbo-BLAST receivers. We show that the EXIT functions which work primarily for AWGN channels are not accurate in giving quantitative performance estimates in a fading environment. A method that copes with this problem and yields reasonably accurate estimates of convergence rate and bit-error-rate is proposed. The performance of different Turbo-BLAST receivers is compared in both single-cell and multicell scenarios.

## I. INTRODUCTION

The Bell-labs space-time layered architecture (BLAST) [2] is one of the advanced signal processing techniques developed for high-rate multiple-input multiple-output (MIMO) systems, which uses decision-feedback multiuser detection (MUD) and can achieve a hefty portion of the predicted capacity. Recently, the iterative turbo principles have been studied for the BLAST system to approach MIMO capacity in noise-limited environments and mitigate the high complexity of optimal processing [1], [3]–[5]. In realistic cellular communications, co-channel interference (CCI) is typically the dominant channel impairment and greatly diminishes the predicted MIMO capacity. In a recent work [1], various multiuser detection (MUD) techniques have been explored in conjunction with Turbo-BLAST to combat the CCI and significantly improve the performance of MIMO systems in a multicell structure.

In this paper, we analyze the performance of the Turbo-BLAST receiver in both noise-limited and interference-limited MIMO systems with the extrinsic information transfer (EXIT) chart, which was first proposed by ten Brink to study the convergence behavior of turbo decoding [6], [7]. As a suitable measure for additive white Gaussian channels, the EXIT Chart is not accurate in giving quantitative performance estimates of iterative receivers in ergodic fading channels. We propose a method which eliminates this difficulty and yields reasonably accurate estimates of convergence rate and bit-error-rate (BER) in fading channels.

The rest of the paper is organized as follows. Section II gives a brief introduction of the Turbo-BLAST receiver and several multiuser detection schemes of interest. Section III and section IV present the EXIT chart analysis of the Turbo-BLAST receiver for the single-cell and multicell cases respectively. Section V contains the conclusions.

## II. TURBO-BLAST MIMO RECEIVERS

### A. Single-Cell Scenario

Consider an  $N_t \times N_r$  MIMO system given by

$$\mathbf{y} = \mathbf{H}\mathbf{x} + \mathbf{n}, \quad (1)$$

where  $\mathbf{y}$  is the received vector,  $\mathbf{x}$  is the transmitted vector constrained to have overall power  $E\{\mathbf{x}^H\mathbf{x}\} \leq P$ ,  $\mathbf{H}$  is the channel matrix, whose entries are i.i.d. normalized complex Gaussian variables; and  $\mathbf{n}$  is circularly symmetric Gaussian background noise with mean zero and covariance matrix  $\sigma^2\mathbf{I}$ . The signal-to-noise ratio is given by  $\rho = P/\sigma^2$ .

The Turbo-BLAST structure is depicted in Fig.1. At the transmitter, the information bits are encoded, interleaved, demultiplexed into  $N_t$  substreams, which are symbol-mapped individually and transmitted. At the receiver, the entire data stream is processed iteratively between a demodulation stage and a decoding stage. The demodulator uses the *a priori* information  $L_{a1}$  and the channel output to produce the extrinsic information  $L_{e1}$ , which is deinterleaved and becomes the *a priori* information  $L_{a2}$  of the decoder. The decoder then uses MAP algorithm to produce the extrinsic information  $L_{e2}$ , which is interleaved and becomes the *a priori* information  $L_{a1}$  of the demodulator. Either Maximum-Likelihood (ML) detection or Parallel-Interference-Cancellation (PIC) detection can be used in the demodulation stage. Due to the space limit, a detailed description of the ML and the PIC detector is omitted here, but can be found in [1].

### B. Multicell Scenario

Next, we consider a multicell system [1] given by

$$\mathbf{y} = \mathbf{H}\mathbf{x} + \sum_i \mathbf{H}_{ifi} \cdot \mathbf{x}_{ifi} + \mathbf{n}, \quad (2)$$

where the subscript “*if*” denotes interference. The channel matrix  $\mathbf{H}$  and  $\mathbf{H}_{ifi}$  are independent and have normalized

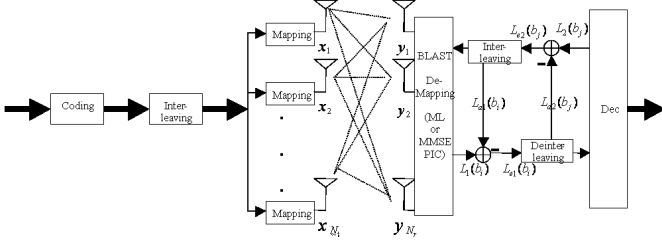


Fig. 1. Structure of Turbo-BLAST

complex Gaussian entries. The transmitted signals from all users are assumed to be of the same format with power  $P_{ifi} = E[\mathbf{x}_{ifi}^H \mathbf{x}_{ifi}] \leq P$ , where the common large scale fading is absorbed in  $P_{if}$ . The signal-to-interference ratio (SIR) is given by  $\eta = P / \sum_i P_{ifi}$ . Since maximum-likelihood joint detection of all cells is prohibitive, suboptimal linear MUD schemes that serve as a preprocessing stage to suppress co-channel interference are of interest, such as the linear MMSE MUD and the channel-shortening (CS) MUD [1].

### C. Important Factors

Before proceeding we briefly discuss the factors that affect the performance of Turbo-BLAST receivers:

- 1) Modulation cardinality and constellation labeling
- 2) Encoding scheme
- 3) Detection scheme
- 4) Signal-to-noise ratio (SNR) and/or signal-to-interference ratio (SIR)
- 5) Number of transmit and receive antennas

Throughout the paper we use 4-QAM to avoid high detection complexity. It is known that certain constellation labeling schemes (such as natural mapping) achieves better performance than Gray mapping in iterative detection and decoding (IDD) systems, which is represented by a steeper detection function with a higher ultimate mutual information value [8]. In this paper we adopt Gray mapping since it facilitates some analytical results. It has also been shown that the plain convolutional outer code achieves convergence with lower SNR thresholds than the turbo code in IDD systems [9]. In this paper we use a rate 1/2 convolutional code with generator polynomial (7,5) for its simplicity, and the block length is 384 bits. The rest of the paper is focused on factors 3), 4) and 5): we study the relative performance of various detection schemes, their BER performance at different SNR/SIR values, and the impact of the number of transmit and receive antennas.

## III. EXIT CHART ANALYSIS OF SINGLE-CELL TURBO-BLAST RECEIVERS

### A. EXIT Chart of Single-Cell Turbo-BLAST Receivers

Let  $I_a = I(b; L_a)$  denote the mutual information between the *a priori* information and the code bits, and  $I_e = I(b; L_e)$

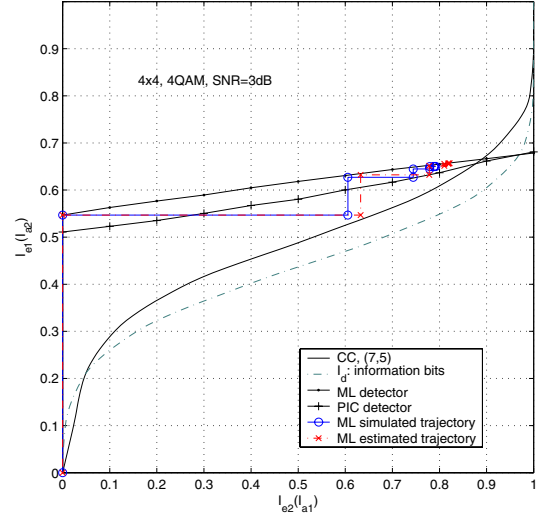


Fig. 2. EXIT chart and trajectories of Turbo-BLAST receiver in single-cell scenario: 4x4, SNR=3dB

denote the mutual information between the extrinsic information and the code bits. The extrinsic information transfer function of a soft-in-soft-out (SISO) component is a mapping of  $I_a$  to  $I_e$  values given a set of parameters. To generate the EXIT function, consistent Gaussian random variables [10] are used to approximate the *a priori* information, i.e. the mean  $\mu_a$  and the variance  $\sigma_a^2$  is related by  $\mu_a = \sigma_a^2/2$ , such that  $I_a$  is a monotonically increasing function of the single parameter  $\sigma_a$ , denoted by  $J(\sigma_a)$ :

$$J(\sigma_a) = 1 - \int_{-\infty}^{+\infty} \frac{e^{-\frac{(l-\sigma_a^2/2)^2}{2\sigma_a^2}}}{\sqrt{2\pi}\sigma_a} \log_2(1 + e^{-l}) dl, \quad (3)$$

and is thus invertible. The EXIT chart of the Turbo-BLAST receiver consists of the EXIT functions of both the detector and the decoder, with axes of the decoder curve reversed. The trajectory of detection and decoding is represented by a zig-zag path on the EXIT chart.

Assume quasi-static block fading, i.e., the channel matrix  $\mathbf{H}$  is fixed for one data block. For MIMO fading channels, the mutual information  $I_e$  should be averaged over all channel realizations:

$$I_e = E_H[I(b; L_e | H_i)], \quad (4)$$

and so does the trajectory. The EXIT functions of the ML and the PIC detector, as well as the simulated average trajectory of the Turbo-BLAST receiver with the ML detector in a  $4 \times 4$  single cell at SNR=3dB are shown in Fig.2. It can be seen from the EXIT functions that the ML detector yields slightly better extrinsic output than the PIC detector, except for the point of  $I_{a1} = 1$ , where both detectors yield the same value of  $I_{e1}$  with perfect *a priori* information. At this point, the interference is completely removed from the received signal.

For AWGN channel, the trajectory matches the EXIT functions asymptotically (as the block length goes to infinity) and the intersection of the detector and decoder functions indicates the termination of the trajectory. For fading channels, however, a considerable discrepancy between the simulated trajectory and the EXIT functions can be observed from Fig.2. We notice that the trajectory does not match the decoder function, but matches the detector function roughly. This means the extrinsic output of the detector in Rayleigh fading channels cannot be approximated by consistent Gaussian variables.

Some analytical results can be obtained for the the extrinsic output of the PIC detector under a fixed channel realization: for BPSK, the extrinsic output is consistent Gaussian with mean  $\frac{2\mu_k^2}{\nu_k^2}$  and variance  $\frac{4\mu_k^2}{\nu_k^2}$ ; for 4-QAM with Gray mapping, the extrinsic output is consistent Gaussian with mean  $\frac{4\mu_k^2}{\nu_k^2}$  and variance  $\frac{8\mu_k^2}{\nu_k^2}$ , where  $\mu_k$  and  $\nu_k^2$  denote the mean and variance of the output of the MMSE filter (see III.B of [1]). Simulations show that the extrinsic output of the ML detector and other modulation schemes is also well-approximated by consistent Gaussian distributions under a fixed channel realization. However, note that the average value of the output of the PIC detector  $\mu_k = \mathbf{w}_k^H \mathbf{h}_k$  varies according to the channel realization, and as a result, the pdf of the detector output in a fading channel is not a consistent Gaussian distribution.

For a fixed channel realization, the detector output is approximately consistent Gaussian, so the trajectory matches the detector and the decoder functions asymptotically. Let  $I_{e1,n}(H_i)$  denote the  $I_{e1}$  value after the  $n$ -th iteration for channel realization  $H_i$ . Then, the  $I_{e1}$  value after the  $n$ -th iteration averaged over all channel realizations is  $\bar{I}_{e1,n} = E_H[I_{e1,n}(H_i)]$ . Similarly define  $I_{e2,n}(H_i)$  and  $\bar{I}_{e2,n}$ . It is easily seen by Jensen's inequality that  $I_{e2}(\bar{I}_{e1,n}) \neq \bar{I}_{e2,n}$ , unless the decoder function  $I_{e2}(I_{a2})$  is a straight line. The extrinsic output of the decoder, on the other hand, is not affected by the channel realizations, so the decoder output can still be approximated by consistent Gaussian variables in fading channels.

### B. Estimating the Average Trajectory

Since the average trajectory does not match the EXIT functions in the fading channel, EXIT functions can only be used to obtain some qualitative results, such as the relative performance of various detection schemes, and the impact of certain system parameters on the performance of the Turbo-BLAST receiver. However, it is often necessary and instructive to obtain some quantitative results, such as the estimates of the number of iterations required for convergence, the BER performance and the SIR/SNR thresholds to achieve a certain BER. EXIT functions are not accurate in giving these results for fading channels, and one has to resort to the average trajectory for an accurate estimation. Generating the average trajectory, nevertheless, requires running the full detection-decoding process.

As a matter of fact, the average trajectory can be *predicted* without free-running the iterative receiver. Since for a fixed channel realization  $H_i$ , the trajectory matches the detector and the decoding functions asymptotically, the trajectory under one channel realization can be predicted from its EXIT functions. The detector function  $I_{e1}(I_{a1}|H_i)$  and the decoder function  $I_{e2}(I_{a2}|H_i)$  under channel realization  $H_i$  are usually generated as piece-wise linear functions. For example, we use a preset of values  $I_a = \{0, 0.1, 0.2, \dots, 0.9, 1\}$ , and find the corresponding  $I_e$  values. The EXIT function is obtained by connecting the adjacent points of  $(I_e, I_a)$  with linear segments, whose mathematical expressions are trivial to obtain. Therefore, the mutual information of the detector output after the first iteration is  $I_{e1,1}(H_i) = I_{e1}(0|H_i)$ , and the mutual information of the decoder output after the first iteration is  $I_{e2,1}(H_i) = I_{e2}(I_{e1,1}|H_i)$ , where  $I_{e2}(I_{a2}|H_i)$  is the expression of the linear segment in the decoder curve corresponding to the interval  $I_{e1,1}(H_i)$  falls in. Similarly, the values for the  $n$ -th iteration can be iteratively found by  $I_{e1,n}(H_i) = I_{e1}(I_{e2,n-1}|H_i)$  and  $I_{e2,n}(H_i) = I_{e2}(I_{e1,n}|H_i)$ . The average trajectory is then found by averaging  $I_{e1,n}$  and  $I_{e2,n}$  over all channel realizations. Note that we only need to generate the decoder function once as it is not affected by channel realizations. The above is done at the same time of generating EXIT functions, and predicting the average trajectory only adds negligible complexity to the process.

In Fig.2, the estimated average trajectory of the Turbo-BLAST receiver with ML detection obtained using the above method is shown. There still exists noticeable discrepancy between the simulated and estimated trajectory. This is due to the small block length, which makes the extrinsic information gets correlated with increasing iterations, and the actual mutual information is slightly lower than that predicted from EXIT curves even for a fixed channel realization. A better agreement between the estimated and the simulated trajectory can be obtained when the block length is increased.

### C. Estimating the BER

Besides the LLR values of the code bits, the decoder also computes the LLR value of the information bits, denoted by  $L_d$ , at each iteration, and a decision is made according to  $\hat{d} = [1 + \text{sgn}(L_d)]/2$ . The same approach of predicting the average trajectory can be used to predict the average mutual information  $I_d$  between the information bit  $d$  and the LLR value  $L_d$  after an arbitrary number of iterations.

As we discussed earlier, the output of the MAP decoder can be roughly approximated by consistent Gaussian variables with variance  $\sigma_d^2$ . We can obtain  $\sigma_d$  for a known  $I_d$  as

$$\sigma_d = J^{-1}(I_d), \quad (5)$$

where  $J^{-1}(\cdot)$  denotes the inverse function of (3). Thus the BER of the information bit is approximated by

$$P_b = Q\left(\frac{\mu_d}{\sigma_d}\right) = Q\left(\frac{\sigma_d}{2}\right). \quad (6)$$

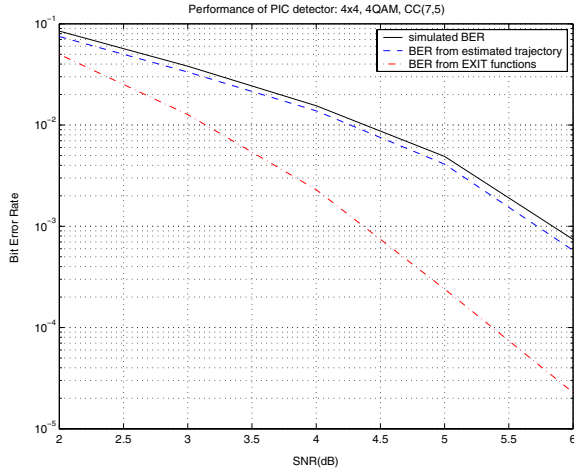


Fig. 3. Comparison of simulated BER, BER obtained from estimated trajectory, and BER obtained from EXIT functions

We can then estimate the BER after an arbitrary number of iterations from the estimated  $I_d$  values without going through the iterations. In Fig.2, another EXIT function,  $I_d-I_{e1}$  with axes reversed is shown. If we predict from EXIT functions directly, the ultimate  $I_d$  value is 0.9620 (the  $I_d$  value on the  $I_d-I_{e1}$  curve corresponding to the  $I_{e1}$  value at the intersection of the ML detector function and the decoder function). Using (5) and (6), we obtain BER=9.80e-3. The  $I_d$  value after convergence (beyond which  $I_d$  hardly increases) estimated with our method is 0.8989, from which we obtain BER=2.66e-2. The simulated BER is 2.74e-2. Therefore our method is more accurate.

As another example, Fig.3 shows the BER-SNR curves of the Turbo-BLAST receiver with the PIC detector in a  $4 \times 4$  single cell, with the three curves corresponding to simulated BER, BER estimated by our method and BER estimated directly from the EXIT functions respectively. Clearly the BER values estimated directly from EXIT functions are much too optimistic, while our method yields reasonably accurate BER estimates down to 1.0e-3.

#### IV. EXIT CHART ANALYSIS OF MULTICELL TURBO-BLAST RECEIVERS

##### A. EXIT Chart and BER Analysis of Multicell Turbo-BLAST Receivers

In a multicell scenario, the choice and combination of intracell MUD and intercell MUD schemes introduced in Section II could yield a number of detector structures. In this section we study the performance of four detector structures:

- 1) MMSE+ML: Linear MMSE MUD followed by ML MUD within the desired cell.
- 2) CS+ML: Channel Shortening MUD followed by ML MUD within the desired cell.
- 3) MMSE+PIC: Note that for a single substream, intracell interference and intercell interference take the same role and can be suppressed by the same MMSE approach.

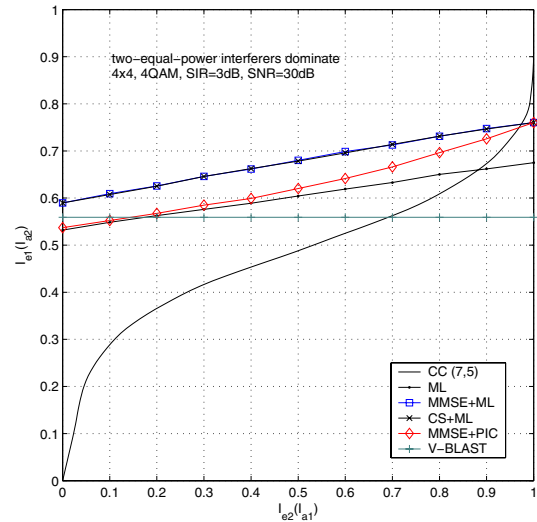


Fig. 4. EXIT chart of multi-cell Turbo-BLAST receivers when two equal power interferers dominate: 4x4, SIR=3dB, SNR=30dB

Thus the two steps can be combined in a single MMSE filter:

$$\mathbf{w}_k = (\mathbf{h}_k \mathbf{h}_k^H + \mathbf{H}_k \mathbf{Q} \mathbf{H}_k^H + \sum_i \frac{P_{if_i}}{P} \mathbf{H}_{if_i} \mathbf{H}_{if_i}^H + \frac{N_t}{\rho} \mathbf{I})^{-1} \mathbf{h}_k. \quad (7)$$

- 4) ML: Only ML MUD within the desired cell is used, and the co-channel interference is treated as Gaussian noise.

Ideally, in the multicell scenario, when SNR and SIR are fixed, the expectation of mutual information between the code bit and the extrinsic information should be carried over all choices of  $\mathbf{H}$ ,  $\mathbf{H}_{if}$ , and  $P_{if}$ . To simplify the problem, we remove the last expectation and only compute the average mutual information under some typical interferer-signal-strength distributions [1], and we found that the EXIT chart is almost invariant to the different interferer-signal-strength distributions.

The EXIT chart for two-equal-power-dominant-interferer case, i.e.,  $P_{if1} = P_{if2} = 4P_{if3} = 4P_{if4}$ , is depicted in Fig.4, where 4 transmit and 4 receive antennas, SIR=3dB and SNR=30dB are used (representing a relatively adverse channel). The EXIT function of coded V-BLAST [1] without ordering is also shown to serve as a comparison. In generating the EXIT function we use the first detected substream of coded V-BLAST, which is a good approximation of the average performance of coded V-BLAST without ordering [11]. Several observations can be drawn from the figure: 1) MMSE+ML and CS+ML have essentially the same (but not identical) performance. This is as expected because both are linear filters which maximizes SINR: MMSE MUD maximizes SINR of each substream, while CS MUD maximizes SINR of all the substreams within the desired cell. 2) The MMSE+PIC yields lower mutual information than the above two schemes at the beginning, but its steeper transfer function

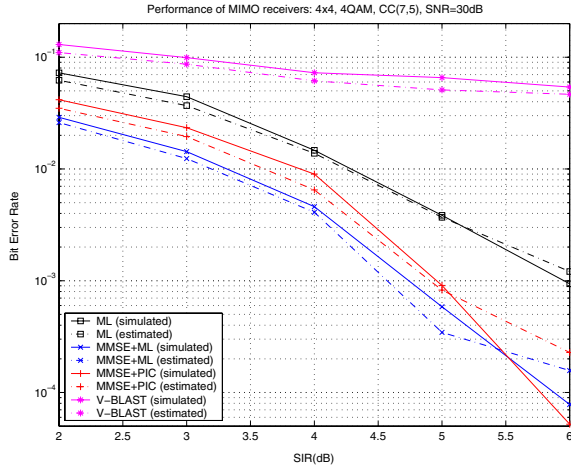


Fig. 5. Simulated and estimated performance of MIMO receivers when two equal power interferers dominate: 4x4, SNR=30dB

enables it to converge to the same point as MMSE+ML and CS+ML with perfect *a priori* information. 3) The ML detector function does not converge to the same point as the above three schemes with perfect *a priori* information, since the interference cannot be completely removed. 4) The coded V-BLAST detector function intersects with the decoder function at a significantly lower mutual information value than the other detector functions do. Note that for the special case of 4QAM and Gray mapping, the extrinsic information of coded V-BLAST is independent on the *a priori* information due to the independence between the in-phase and quadrature parts, so its detector function is a horizontal line.

The  $I_d$  values of these schemes after each iteration are estimated using the method in Section III. C., and the BER of each scheme are then estimated from the  $I_d$  values after convergence. The simulated BER, along with the estimated BER are plotted in Fig.5. It can be seen that the BER of MMSE+PIC approaches the BER of MMSE+ML, and both intercell MUD schemes perform much better than ML when SIR is significant (BER is lowered by one order of magnitude at SIR=6dB). Meanwhile, coded V-BLAST displays a high BER-floor. Since for the same BER requirement, MUD for intercell interference mitigation enables us to work in a worse environment, they have wider applications in practical systems. Note that MMSE+PIC is much simpler than MMSE+ML and CS+ML. The detection component of MMSE+PIC is also simpler than ML, although channel information of interfering users is required. Fig.5 also demonstrates that our method is capable of giving good BER estimates down to  $1.0e-3$ .

### B. Receive Diversity

The receive diversity is much under-exploited in the multi-cell scenario as there are far more transmit antennas than receive antennas. When the SIR and SNR values are fixed, either increasing the number of receive antennas or decreasing the

number of transmit antennas makes the detector function move upward in the EXIT chart, hence better BER performance of the Turbo-BLAST receiver. Decreasing the number of transmit antennas, however, sacrifices the data rate. EXIT chart analysis shows that, by increasing the number of receive antennas from 4 to 6 (4 transmit antennas, SIR=2dB and SNR=30dB), the estimated BER is reduced from  $2.7e-2$  to  $1.0e-3$ . Alternatively, the SIR threshold to achieve a BER of  $1.0e-3$  is reduced from 5.0dB to 2.0dB. Although the number of receive antennas is limited by the size of the receiver equipment, more receive antennas is obviously desirable whenever possible.

### V. CONCLUSION

In this paper, we have used the EXIT chart to analyze several MUD schemes employed by the Turbo-BLAST receiver to combat interference in both single-cell and multicell MIMO systems. We have proposed a method to estimate the average trajectory and the ultimate mutual information in fading channels without free-running the iterative receiver, with which the BER performance of the various detectors is estimated and compared. We have shown that in the interference-limited environment, the low complexity MMSE+PIC achieves similar performance as MMSE+ML and CS+ML, and the intercell MUD schemes largely outperform ML within the desired cell only.

### REFERENCES

- [1] H. Dai, A. F. Molish, and H. V. Poor, "Downlink capacity of interference-limited MIMO systems with joint detection," *IEEE Trans. Wireless Commun.*, vol. 3, pp. 442–453, Mar. 2004.
- [2] G. J. Foschini, "Layered space-time architecture for wireless communication in a fading environment when using multi-element antennas," *Bell Labs Tech. J.*, vol. 2, pp. 41–59, Autumn 1996.
- [3] S. L. Ariyavisitakul, "Turbo space-time processing to improve wireless channel capacity," *IEEE Trans. Commun.*, vol. 48, pp. 1347–1359, Aug. 2000.
- [4] M. Sellathurai and S. Haykin, "Further results on diagonal-layered space-time architecture," in *Proc. IEEE VTC 2001 Spring*, Rhodes, Greece, May 2001.
- [5] A. van Zelst, R. VanNee, and G. A. Awater, "Turbo-BLAST and its performance," in *Proc. IEEE VTC 2001 Spring*, Rhodes, Greece, May 2001.
- [6] S. ten Brink, "Convergence of iterative decoding," *IEEE Electronic Letters*, vol. 35, pp. 806–808, May 1999.
- [7] —, "Convergence behavior of iteratively decoded parallel concatenated codes," *IEEE Trans. Commun.*, vol. 49, pp. 1727–1737, Oct. 2001.
- [8] —, "Designing iterative decoding schemes with the extrinsic information transfer chart," *AEU Int. J. Electron. Commun.*, pp. 389–398, 2000.
- [9] S. ten Brink and B. M. Hochwald, "Detection thresholds of iterative MIMO processing," in *Proc. IEEE ISIT*, Lausanne, Switzerland, 2002.
- [10] T. Richardson and R. Urbanke, "The capacity of low-density parity-check codes under message-passing decoding," *IEEE Tran. on Inform. Theory*, vol. 47, pp. 599–618, Feb. 2001.
- [11] P. Narayan and M. Varanasi, "Analysis of decision feedback detection for MIMO rayleigh fading channels and optimization of power and rate allocations," *IEEE Trans. Inform. Theory*, in press.
- [12] X. Wang and H. V. Poor, "Iterative (turbo) soft interference cancellation and decoding for coded CDMA," *IEEE Trans. Commun.*, vol. 47, pp. 1046–1061, July 1999.
- [13] K. Li and X. Wang, "EXIT chart analysis of turbo multiuser detection," *IEEE Trans. Wireless Commun.*, in press.